Selective oxidation of methane to formaldehyde on supported molybdate catalysts

M.A. Bañares and J.L.G. Fierro [1]

Instituto de Catálisis y Petroeoquímica, CSIC, Campus UAM, Cantoblanco, 28049 Madrid, Spain

Received 14 September 1992; accepted 4 November 1992

A series of silica-supported molybdena catalysts with variable molybdenum content has been prepared and tested in the selective oxidation of methane to formaldehyde. The nature of the supported oxide phases has been studied by Fourier transform IR of chemisorbed NO molecule, X-ray photoelectron spectroscopy, UV-Visible reflectance and X-ray diffraction techniques. The results show that molybdenum oxide is highly dispersed on the silica at low molybdenum concentrations where two-dimensional polymolybdates are developed. Three-dimensional MoO_3 crystals grow in the region of high molybdenum concentrations. The analysis of the combined data suggests that there is a close relationship between methane conversion and formaldehyde selectivity and the presence of highly dispersed polymolybdate structures on the silica surface.

Keywords: Methane partial oxidation; silica-supported molybdate catalysts; catalyst characterization; FTIR of chemisorbed NO; photoelectron spectroscopy

1. Introduction

The conversion of methane into C_1 oxygenates (formaldehyde and methanol) in a single catalytic step constitutes one of the processes of greatest chemical and technological relevance. As a result of its importance, many attempts have been made to convert methane into C_1 oxygenates [1–7]. However, the heterogeneous reactions occur at rather high temperatures, typically 870 K, as the high stability of the CH_4 molecule imposed by the sp^3 hybridization of the C atom must be overcome. As the subsequent combustion reactions of these intermediates are much easier than the activation of methane, the formation of oxygenates appears highly improbable. However, surprisingly a common feature of the attempts to find selective catalysts for this purpose has been that it does seem possible to produce oxygenates separately and with reasonable selectivity.

[1] To whom correspondence should be addressed.

The catalysts used for the selective oxidation of methane are constituted of redox oxides supported on silica of moderate or high surface area [8–15] or even on zeolites [16,17]. Also molybdenum oxometallates have been reported as active and selective for this reaction [18,19]. In particular, molybdenum oxide appears very attractive owing to its moderate activity, high selectivity and its relative stability under the severe temperatures at which the reaction is operative. However, there is no consensus of opinion as to whether a structure–activity relationship exists for this type of catalysts. For all of these reasons, MoO_3/SiO_2 catalysts have been selected in this study with the aim of determining whether such a correlation exists in the selective oxidation of methane. To achieve this goal the molybdenum concentration was varied over a wide range and the resulting catalysts were characterized by X-ray photoelectron spectroscopy, Fourier transform IR of chemisorbed NO probe, diffuse reflectance and X-ray diffraction. The combined analysis of the data and that of activity and selectivity allow us to establish a structure–activity relationship.

2. Experimental

A commercial silica (Aerosil Mox-80), particle size 30 nm, BET area 86 $m^2\ g^{-1}$ and composition $SiO_2 > 98.3\%$, $Al_2O_3 = 0.3–1.3\%$, $Fe_2O_3 < 0.01\%$ and $Na_2O \approx 0.05\%$, was used as carrier. This was impregnated with aqueous ammonium heptamolybdate (Merck) solutions in appropriate amounts so as to yield Mo concentrations in the range 0.3–3.5 Mo atoms per nm of silica surface. The impregnates were dried at 383 K and calcined in two steps: 2 h at 623 K and 5 h at 923 K. Prior to use the catalysts were pelleted and sieved to sizes 0.42–0.50 mm. They are referred to hereafter as Mox, where x denotes the surface concentration in Mo atoms per square nanometer of silica carrier.

For the infrared experiments very thin self-supporting wafers (8–10 mg cm^{-2}) were prepared and mounted in a special infrared cell assembled with greaseless stopcocks and KBr windows. The samples were firstly purged in a He flow while heating to 790 K, then reduced in a H_2 flow (60 $cm^3\ min^{-1}$) at this temperature for 1 h. After reduction, the catalysts were outgassed in high vacuum for 0.5 h and then cooled down to room temperature. Subsequently, they were exposed to 4 kN m^{-2} (133.33 N m^{-2} = 1 Torr) NO gas and the IR spectra recorded on a Nicolet 5ZDX FT spectrophotometer working with a resolution of 4 cm^{-1}.

The X-ray photoelectron spectra (XPS) were recorded with a Leybold LHS 10 spectrometer equipped with a Mg Kα X-ray excitation source ($h\nu$ = 1253.6 eV). The samples were turbopumped to $\approx 10^{-3}$ N m^{-2} before they were moved into the analysis chamber. The residual pressure in this ion pumped chamber was maintained below 5×10^{-7} N m^{-2} during data acquisition. 20 eV energy regions of the photoelectrons of interest were signal-averaged for a number of scans in order to obtain good signal-to-noise ratios at reasonable acquisition times.

Although surface charging was observed in all samples, accurate (± 0.2 eV) binding energies (BE) could be determined by charge referencing with the Si 2p peak, assigned a BE value of 103.4 eV.

Diffuse reflectance spectra were recorded on a Varian Cary 210 spectrophotometer equipped with an integrator accessory. Discs of the samples with ≈ 1 mm thickness were prepared in order to yield the reflectance at infinite thickness (R_∞). The electronic spectra were then evaluated according to the Kubelka–Munk–Schuster (KMS) function ($F(R_\infty)$). The X-ray diffraction patterns were recorded with a Siemens Kristalloflex D500 diffractometer equipped with a copper X-ray tube operated at 40 kV and 20 mA, a nickel filter and a graphite receiving monochromator. The scans for the calcined, reduced and activated catalysts were made over the range 5–65 2Θ at 0.05° intervals. The crystal phase composition of the samples was determined by comparison with standard ASTM files.

Activity measurements were carried out at atmospheric pressure in a fixed-bed quartz microcatalytic reactor by cofeeding CH_4 (99.95% vol) and O_2 (99.98% vol) without diluent. The $CH_4:O_2$ ratio was adjusted in the range 5–15 molar by means of mass flow controllers (Brooks) and the methane residence time was adjusted to 1 and 6 s. The reactor effluents were analyzed by on-line GC using a Konik 3000HR gas chromatograph fitted with a TCD. Chromosorb 107 and Molecular Sieve 5A packed columns using a column isolation analysis system were used in this study.

3. Results and discussion

The overall infrared spectra are quite complex since the silica lattice displays an intense overtone in the spectral region 1900–1650 cm^{-1} where NO bands usually appear, therefore masking the IR absorption of NO molecule in this region. To avoid this, the spectrum of the bare catalyst was subtracted from that of the catalyst exposed to NO. All infrared spectra show the characteristic doublet at ≈ 1810 and 1710 cm^{-1} assigned to the symmetric and antisymmetric NO fundamental stretching vibrations, respectively, of paired $(NO)_2$ molecules adsorbed as dinitrosyl or dimeric structures [20] on reduced Mo sites, probably Mo^{4+}. For illustrative purpose only one of these spectra is shown in the inset of fig. 1. Fig. 1 displays the integrated intensity of the band at ≈ 1710 cm^{-1}, normalized to the BET area, as a function of Mo concentration. The band intensity increases sharply in the region of low Mo loadings, attaining a maximum at ≈ 1 Mo nm^{-2} then decreases. As the extent of reduction appears to be almost the same for all catalysts [21], the intensity decrease observed for $x = 1.9$ and 3.5 may well be related to a lower Mo oxide dispersion. Therefore, the observed intensities could be taken as a measure of molybdena exposure at the catalyst surface.

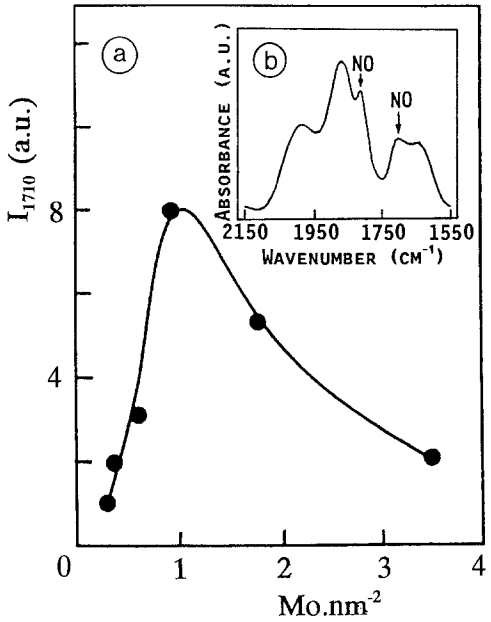

Fig. 1. (a) Influence of the Mo concentration on the integrated intensity (normalized) of the IR band of NO at ≈ 1710 cm^{-1}; (b) the inset illustrates the total spectrum (without background subtraction) of chemisorbed NO on the reduced catalyst $x = 1.0$.

The XP spectra showed the characteristic Mo 3d doublet with a poor resolution and BE values for the most intense Mo $3d_{5/2}$ peak at 231.5–232.1 eV (table 1), somewhat below that reported for MoO_3 [22]. These facts reveal the presence of partially reduced $Mo^{\delta+}$ $(5 < \delta < 6)$ species generated upon X-ray irradiation inside the spectrometer. Consistent with this is the intense blue colour of samples (Kihlborg phases) after analysis due to formation of oxygen deficient structures through edge-sharing MoO_6 octahedra upon losing a small proportion of oxygen atoms from the corners. In order to obtain an estimate of the dispersion of MoO_3 the Mo/Si XPS intensity ratios have been calculated. To account for changes of BET areas, these values were normalized and

Table 1
MoO_3/SiO_2 catalysts characteristics

Mo (nm^2)	S_{BET} (m^2/g)	BE Mo $3d_{5/2}$ (eV)	I_{Mo}/I_{Si}
0.3	77	231.5	3.0
0.4	69	232.1	3.7
0.6	68	231.7	5.9
1.0	69	231.8	6.5
1.9	40	231.9	12.7
3.5	42	232.0	12.4

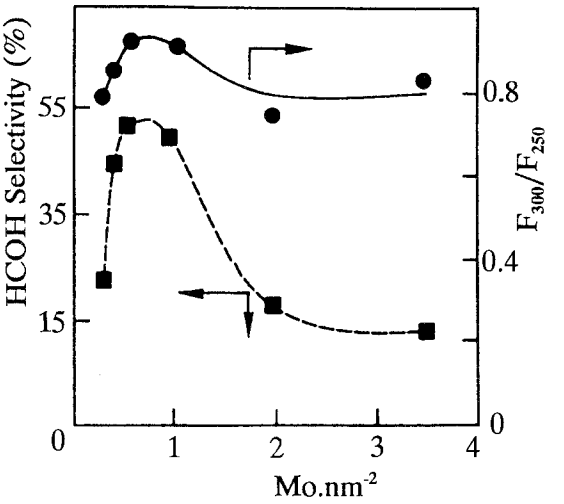

Fig. 2. Influence of the Mo concentration on HCOH selectivity (■) (863 K, $CH_4/O_2 = 5$, CH_4 conversion = 1.0%) and on the remission functions F_{300}/F_{250} (●).

collected in table 1. The almost linear increase of the Mo/Si XPS intensity ratio up to $x = 1.9$ indicates a uniform and relatively well dispersed Mo oxide phase. The drastic decrease of this ratio for the catalyst $x = 3.5$ indicates MoO_3 clustering.

The electronic spectra of calcined catalysts showed two bands at 230–270 and 270–305 nm, corresponding to Mo^{6+} ions surrounded by oxygen anions in T_d and O_h symmetries, respectively. The latter band at 270–305 nm indicates the presence of M–O–Mo bridges in polymolybdate structures [21,23]. The remission functions at 300 and 250 nm (F_{300}/F_{250}) have been calculated from the spectra and plotted in fig. 2 as a function of the Mo concentration. The increase of this ratio with Mo concentration up to $x = 0.6$ Mo suggests, in agreement with literature findings [23], a parallel increase in the degree of polymerization, leading to lesser and lesser dispersed molybdenum oxide phase. Consistent with this interpretation is the observation of X-ray diffraction lines of MoO_3 phase for $x = 3.5$, for which the size of MoO_3 crystallites is high enough to be detected by this technique. The methane partial oxidation with molecular oxygen yields primarily HCOH and carbon oxides, with minor amounts of methanol, hydrogen and dimerization products (ethane). The activity of the catalysts increased, as expected, with increasing reaction temperature; however, the HCOH selectivity decreased with increasing methane conversion with the subsequent increase in CO_x yields and, to a lesser extent, ethane formation. Similarly, the conversion levels of both methane and oxygen can be reasonably increased by increasing the methane residence time (table 2). It is noteworthy that the HCOH and CO selectivities always followed an opposite trend: while HCOH selectivity increased (decreased) that of CO decreased (increased). This fact indicates that

Table 2
Methane oxidation on Mo0.6 [a]

τ (s)	Conversion (%)		Selectivity (%)				
	CH_4	O_2	HCHO	CO	CO_2	C_2H_6	CH_3OH
1.0	0.6	6.0	51.3	46.4	1.3	0.6	0.1
2.0	1.9	13.2	28.6	68.0	3.1	0.2	0.1
3.0	2.8	21.3	21.0	75.4	3.6	0.1	< 0.1
4.7	4.6	38.0	10.1	80.5	9.4	–	t

[a] Reaction temperature, 863 K. $CH_4/O_2 = 5$ molar.

HCOH is a primary product while CO is a secondary product. Moreover, the transformation of HCOH into CO seems to take place mainly in the gas phase, since HCOH selectivity was enhanced by a factor ≈ 3 by decreasing the post reaction volume [13]. The origin of CO_2 is, however, much more complex. Using an oxygen-18 labeling we recently demonstrated [14] that CO_2 can be formed through three different routes: (i) direct combustion from CH_4 molecule at catalyst surface, (ii) oxidation of CO by the unreacted oxygen, and (iii) water–gas shift ($CO + H_2O \rightleftharpoons CO_2 + H_2$) reaction. On the basis of hydrogen concentrations detected in the reactor effluents it has been established that type (iii) contribution represents only about one fifth of the overall CO_2 amount [24].

It has been shown that the catalyst activity is strongly influenced by molybdenum concentration. Fig. 2 shows that HCOH selectivity, obtained at 863 K and constant methane conversion ($x_{CH_4} = 1.0$), increases sharply in the low composition range, attaining a maximum close to $x = 1$ and decreasing for $x = 1.0$–3.5. A similar trend has already been observed for methane conversion at this temperature.

The XPS data and the integrated absorbance of the 1710 cm^{-1} IR band due to chemisorbed NO on reduced catalysts indicate that molybdenum oxide is rather well dispersed up to $x = 1.0$. Moreover, the absorption band in the energy region 270–305 nm, associated with polymeric molybdate structures, and the increase of the F_{300}/F_{260} ratio, suggests that MoO_4^{2-} tetrahedra interact with each other and this tends to decrease the Mo dispersion. Only at high concentrations ($x = 3.5$) does MoO_3 clustering become important enough to be detectable by XRD. The comparison of activity data with those of infrared and diffuse reflectance reveals a close relationship between the exposure of $Mo^{\delta+}$ sites and formation of polymolybdates and HCOH selectivity and methane conversion.

Acknowledgement

The authors wish to express their gratitude to the CICYT (Spain) for supporting this research (Grant MAT 91-0494). They are also indebted to Dr.

J.A. Anderson for critical reading of this manuscript and Professor M.A. Bañares for the XRD measurements.

References

[1] H.F. Liu, R.S. Liu, K.Y. Liew, R.E. Johnson and J.H. Lunsford, J. Am. Chem. Soc. 106 (1984) 4117.
[2] M.M. Khan and G.A. Somorjai, J. Catal. 91 (1985) 263.
[3] K.J. Zhen, M.M. Khan, C.H. Mak, K.B. Lewis and G.A. Somorjai, J. Catal. 94 (1985) 501.
[4] N.R. Foster, Appl. Catal. 19 (1985) 1.
[5] K. Pitchai and K. Klier, Catal. Rev. Sci. Eng. 28 (1986) 13.
[6] J.S. Lee and S.T. Oyama, Catal. Rev. Sci. Eng. 30 (1988) 249.
[7] M.J. Brown and N.D. Parkyns, Catal. Today 8 (1991) 305.
[8] X. Kuan and J.M. Thomas, J. Chem. Soc. Chem. Commun. (1988) 162.
[9] Y. Barbaux, A. Elamrani and J.P. Bonnelle, Catal. Today 1 (1987) 147.
[10] N.D. Spencer and C.J. Pereira, J. Catal. 116 (1989) 399.
[11] M. Kennedy, A. Sexton, B. Kartheuser, E. McGiolla Coda, J.B. McMonagle and K.B. Hodnett, Catal. Today 13 (1992) 447.
[12] T. Weng and E.E. Wolf, Am. Chem. Soc., Symp. Petr. Chem. Div., Preprints, 37 (1992) 46.
[13] M.A. Bañares and J.L.G. Fierro, Am. Chem. Soc., Symp. Petr. Chem. Div., Preprints, 37 (1992) 1171.
[14] M.A. Bañares, I. Rodríguez-Ramos, A. Guerrero-Ruíz and J.L.G. Fierro, in: *Proc. 9th Int. Cong. on Catalysis*, Budapest 1992, Paper O76, p. 124.
[15] A. Parmaliana, V. Sokolowski, D. Miceli, F. Arena and N. Giordano, Am. Chem. Soc., Symp. Petr. Chem. Div., Preprints, 37 (1992) 1076.
[16] J.R. Anderson and P. Tsai, J. Chem. Soc. Chem. Commun. (1987) 1435.
[17] M.A. Bañares, B. Pawelec and J.L.G. Fierro, Zeolites (1992), in press.
[18] S. Kasztelan, E. Payen and J.B. Moffat, J. Catal. 112 (1988) 320.
[19] S. Kasztelan and J.B. Moffat, in: *Proc. 9th Int. Cong. on Catalysis*, Calgary 1988, eds. M.J. Phillips and M. Ternan (Chemical Institute of Canada, Ottawa, 1988).
[20] J.L.G. Fierro, in: *Spectroscopic Characterization of Heterogeneous Catalysts, Part B, Chemisorption of Probe Molecules*, Vol. 27B, ed. J.L.G. Fierro (Elsevier, Amsterdam, 1990) p. B67, and references therein.
[21] M.A. Bañares and J.L.G. Fierro, An. Quím. 87 (1991) 223.
[22] C.D. Wagner, W.M. Riggs, L.E. Davis, J.F. Moulder and G.E. Muilenberg, *Handbook of X-Ray Photoelectron Spectroscopy* (Perkin Elmer Co., Eden Prairie, 1978).
[23] C. Rocchoccioli-Deltcheff, M. Amirouche, M. Che, J.M. Tatibouet and M. Fournier, J. Catal. 15 (1990) 292.
[24] M.A. Bañares, J.L.G. Fierro and J.B. Moffat, in preparation.